

Observing Unimolecular Dissociation of Metastable Ions in FT-ICR: A Novel Application of the Continuous Ejection Technique

Chuan-Yuan Lin, Quan Chen, Huiping Chen, and Ben S. Freiser*

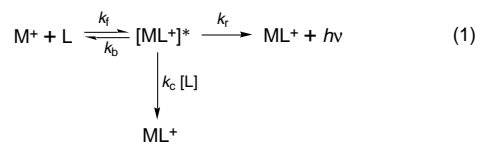
H. C. Brown Laboratory of Chemistry, Purdue University, West Lafayette, Indiana 47907

Received: February 5, 1997; In Final Form: May 2, 1997[⊗]

The application of the continuous ejection technique to observe unimolecular dissociation of metastable organometallic ions in a Fourier transform ion cyclotron resonance (FT-ICR) mass spectrometer is demonstrated. A radio-frequency ejection voltage is continuously applied at a frequency corresponding to the exact mass of a metastable adduct ion, $[\text{MC}_6\text{H}_6^+]^*$ ($M = \text{Cr}$ and Mn), formed in the reactions of Cr^+ and Mn^+ with C_6H_6 . By monitoring the initial metal ion intensity as a function of ion ejection time, metastable ion lifetimes and unimolecular dissociation rate constants are obtained. The bond dissociation energies $D^0(\text{Cr}^+ - \text{C}_6\text{H}_6) = 1.75 \pm 0.1$ eV and $D^0(\text{Mn}^+ - \text{C}_6\text{H}_6) = 1.50 \pm 0.1$ eV are derived from RRKM modeling and are in excellent agreement with other literature values.

Introduction

The study of ion–molecule reactions in the gas phase has been a very active area for over two decades.^{1–13} In particular, there has been an intense interest in low-pressure ion–molecule association reactions.^{14–23} Ion–molecule reactions involve collisions between ions and neutral molecules to form *metastable* adduct ions. In the simplest case, the probability of observing stabilized adduct ions depends on the competition between back-dissociation and stabilization of the metastable adduct ions.^{19–21} Metastable adduct ions can be stabilized by either photon emission or additional collisions,¹⁶ as expressed by reaction 1



where the rate constants are those for adduct formation (k_f), back-dissociation (k_b), collisional stabilization (k_c), and radiative stabilization (k_r).¹⁹

In the low-pressure regime ($\sim 10^{-8}$ Torr in an ion cyclotron resonance (ICR) cell or in interstellar space), where third-body collisional stabilization of the metastable adduct ions is very slow, the metastable ions are stabilized predominantly by emitting infrared photons, a process termed *radiative association* (RA).^{16,20} The role of radiative association reactions in the chemistry of interstellar clouds has long received a great deal of attention by astrochemists and astrophysicists.^{14–18} It is believed that radiative association is an important route in building large molecules and ions in the interstellar environment.

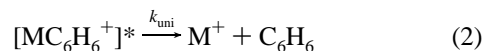
Recently, Dunbar and co-workers have developed a new methodology involving radiative association reactions that allows the determination of ligand/metal ion bond energies.^{20–23} This method is based on the assumption that the rate of producing stabilized adduct ions is a strong function of ligand/metal ion bond energies for moderately sized metal-complex ions.^{19–23} Normally, strongly bound adduct ions have sufficiently long lifetimes to be stabilized and observed experimentally. For weakly bound adduct ions, however, the lifetimes are too short to allow the metastable adduct ions to be stabilized,

and thus, most newborn adduct ions dissociate back to reactants. Therefore, it might be difficult to apply the RA kinetic method to those weakly bound ions, especially to those having few degrees of freedom.

Generally, only stabilized ions can be detected in a Fourier-transform ion cyclotron resonance (FT-ICR) mass spectrometer, since the time required for ion detection in FT-ICR is usually longer than 1 ms. Consequently, metastable ions with lifetimes of several hundreds of microseconds cannot be observed *directly* using standard FT-ICR excitation/detection techniques. Anichich and co-workers have recently demonstrated,^{24,25} however, that the lifetime²⁶ distribution of metastable ions can be obtained using ion cyclotron double-resonance techniques in FT-ICR. Basically, a radio-frequency (rf) ejection voltage is continuously applied at the cyclotron frequency of the selected metastable ions during a constant reaction time. Metastable ions with lifetimes longer than the ion ejection time will be ejected from the ICR cell; those with short lifetimes will dissociate back to reactants prior to ejection. A decrease of the initial reactant ion intensity will be found in the former case, while there is a leveling off at longer ejection times of the initial reactant ion intensity in the latter case. By monitoring reactant ion intensity as a function of ion ejection time, Anichich and co-workers were able to derive the mean lifetime of the metastable ion, $(\text{CH}_3\text{-CNCH}_3^+)^*$, at about $140 \mu\text{s}$.²⁵

Audier and McMahon²⁷ have also applied the continuous ejection technique to reexamine the reaction mechanism of $\text{CH}_3\text{-OCH}_2^+$ with acetone, first reported by Nibbering and co-workers.²⁸ According to their new metastable ion cyclotron resonance (MICR) results, the product distribution strongly depends upon the internal energy of the metastable adduct ion, $[\text{CH}_3\text{OCH}_2^+(\text{CH}_3)_2\text{CO}]^*$. In particular, by sampling at longer lifetimes, they showed that the metastable adduct ions with low internal energies could overcome a central barrier from a covalent intermediate to an electrostatic intermediate and subsequently eliminate H_2CO .

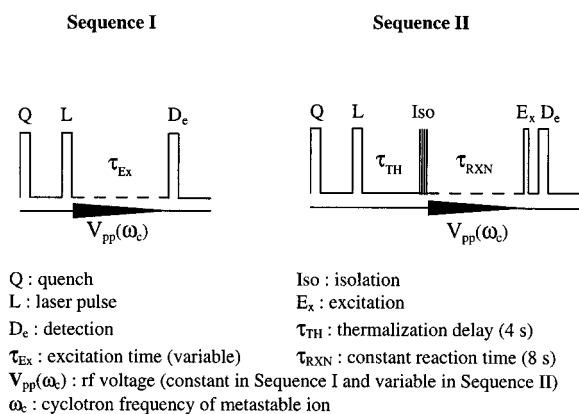
In the present study, we extend the application of the continuous ejection technique^{24,25,28} (i) to obtain the unimolecular dissociation rate constant, k_{uni} , for the chemically activated intermediates, $[\text{MC}_6\text{H}_6^+]^*$ ($M = \text{Cr}$ or Mn), in reaction 2 and (ii) to obtain the bond dissociation energies, $D^0(\text{Cr}^+ -$



* To whom correspondence should be addressed.

[⊗] Abstract published in *Advance ACS Abstracts*, August 1, 1997.

SCHEME 1



C_6H_6) and $D^0(\text{Mn}^+-\text{C}_6\text{H}_6)$, using RRKM modeling.^{29–32} The derived bond dissociation energies are compared to those obtained by Meyer and Armentrout from threshold collision-induced dissociation (CID)³³ and by Lin and Dunbar from the RA kinetic method,²³ in order to evaluate the accuracy of the present approach.

Experimental Section

All of the experiments were performed on a Nicolet (currently Finnigan FT/MS) FTMS-2000 Fourier transform ion cyclotron resonance (FT-ICR) mass spectrometer controlled by an Odyssey data station.^{34,35} A dual cell (each cell being $4.90 \times 4.90 \times 4.90 \text{ cm}^3$) is located in a 3 T superconducting magnet. The high-vacuum chambers are differentially pumped by two separate diffusion pumps and operate at background pressures below 0.6×10^{-8} Torr.

The precursor ion, M^+ ($\text{M} = \text{Cr}$ and Mn), was generated via laser desorption/ionization (LDI) by focusing the fundamental laser beam (1064 nm) of a Nd:YAG laser (Quanta-Ray) onto a pure metal target.³⁶ Benzene was introduced into the ICR cell through a Varian leak valve, and a static pressure was maintained. A Bayard-Alpert ionization gauge was used to monitor pressure. Pressure calibrations were derived using the literature ionization gauge factors,³⁷ followed by a geometry correction using calibration charts obtained from the manufacturer. Temperatures were measured using three thermocouples positioned on the vacuum chamber.

To examine the time required for ion ejection on the FTMS-2000, a series of experiments were performed using sequence I shown in Scheme 1. After generating Cr^+ by LDI, a constant rf excitation voltage was applied differentially to both transmitter plates at the cyclotron frequency of the chromium ion. The Cr^+ intensity was measured at different excitation pulse widths, ranging from several microseconds to milliseconds. The same calibration procedure was also carried out at different rf excitation voltages.³⁸

Sequence II in Scheme 1 shows the experimental sequence used for the continuous ejection experiments. In brief, metal ions were produced by the laser desorption/ionization technique, followed by a time delay of 4 s to cool the metal ions translationally at benzene pressures of $(2-6) \times 10^{-7}$ Torr. Ion isolation was achieved by applying a series of swept double-resonance ejection pulses³⁹ and SWIFT excitation pulses.⁴⁰ An rf ejection voltage (single-frequency mode) was then continuously applied at a frequency corresponding to the cyclotron frequency of the metastable adduct ion, $[\text{MC}_6\text{H}_6^+]^*$, during a constant reaction time of 8 s. The reaction delay was arbitrarily chosen to allow a substantial amount of the metastable adduct ions to be formed. Radio-frequency ejection voltages, V_{pp} peak-

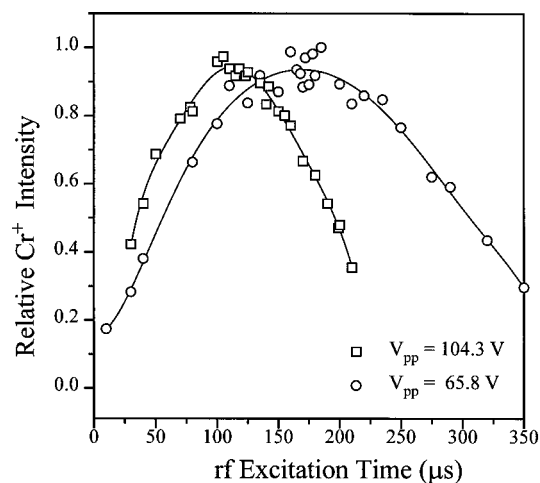


Figure 1. Observed chromium ion intensity as a function of rf excitation time at 104.3 V (squares) and 65.8 V (circles). The solid lines are the polynomial function fits (sixth-order).

to-peak, were measured with an oscilloscope as a function of attenuator setting and were varied from 117 to 1.17 V. The metal ion intensity was monitored using standard FT-ICR excitation/detection techniques.

Results

Calibration of Ion Ejection Time. Figure 1 shows two examples of Cr^+ intensity as a function of rf excitation time at excitation voltages of 104.3 and 65.8 V, using sequence I. The Cr^+ intensity is observed to increase monotonically at short excitation times and reach a maximum, after which the intensity begins to drop. This observation is consistent with those reported by Marshall and McMahon, as detailed in refs 38 and 27. The time to reach the maximum ion intensity (maximum cyclotron radius) corresponds to the minimum time for ion ejection. As seen in Figure 1, the (minimum) ion ejection times were determined to be 112 ± 10 and $170 \pm 15 \mu\text{s}$ at rf excitation voltages of 104.3 and 65.8 V, respectively. The same calibration procedure was also performed at rf excitation voltages of 20.8 and 11.7 V, which gave τ_{Ej} of 650 ± 60 and $1000 \pm 100 \mu\text{s}$, respectively. The open circles in Figure 2 represent the measured ion ejection times at different rf excitation voltages.

Theoretical Calculation of Ion Ejection Time. For ions in a cubic ICR cell, the time required for ion ejection, τ_{Ej} , can be derived from the power absorption (on-resonance) of radio frequency for a charged particle circulating in a high magnetic field;^{41–43} the resulting equation is expressed as

$$\tau_{\text{Ej}} = (d^2/\beta V_{\text{pp}})B \quad (3)$$

where B is the magnetic field strength, V_{pp} is the peak-to-peak rf voltage applied in a dipolar fashion across opposite transmitter plates, d is the cell dimension ($d = 2r$, r is the ion radius), and β is the cell geometry factor ($\beta = 0.72167$ for a cubic cell).⁴³ As can be seen in Figure 2, the measured ion ejection times are quite close to the calculated values, with the average measured values being about 15% greater than the calculated values.

Continuous Ejection Results. In the present study, two benzene/metal ion systems, CrC_6H_6^+ and MnC_6H_6^+ , were investigated using the continuous ejection technique (sequence II). The results are displayed in Figure 3, where the measured metal ion intensity is shown as a function of ion ejection time. Note that the metal ion intensities have been converted to relative ion intensities by normalizing them to those obtained

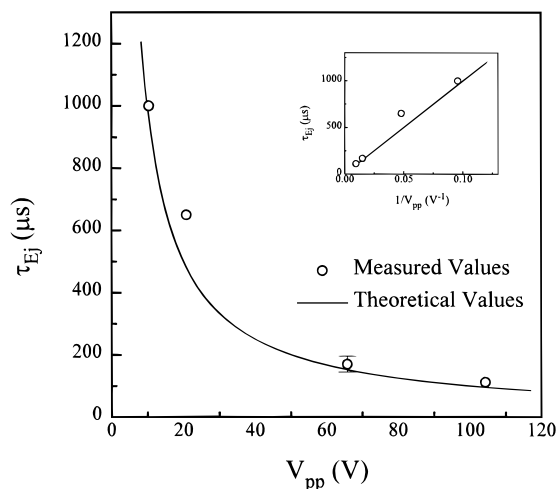


Figure 2. Measured ion ejection times at different rf excitation voltages (open circles). Theoretical values were calculated according to eq 3 with $B = 3$ T, $d = 4.90$ cm, and $\beta = 0.72167$. A plot of ion ejection time vs the inverse of rf voltage is shown in the insert.

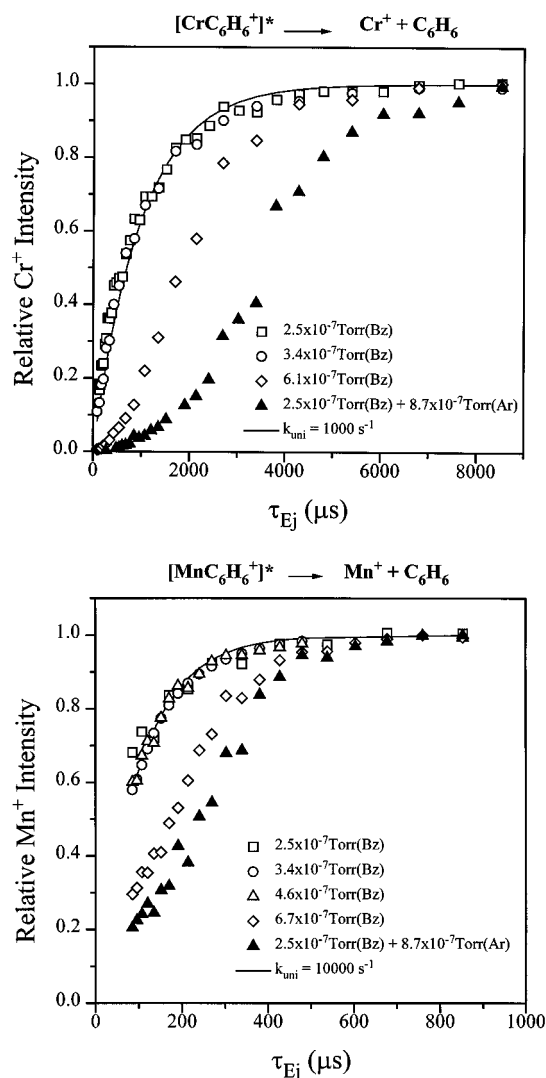


Figure 3. Measured (a) Cr^+ and (b) Mn^+ intensities as a function of ion ejection times at different benzene pressures (open symbols) and with additional Ar collisional gas (solid triangles). The solid line is a simple exponential fit.

without rf ejection voltage during the same reaction period. The x -axis in Figure 3 is the calculated ion ejection time according to eq 3.

As seen in Figure 3, the metal ion intensity levels off at long ion ejection times (low rf voltages) and starts to fall off as the time required for ion ejection decreases (high rf voltages). The decrease of metal ion intensity as the rf voltage increases is due to a reduction in the extent of back-dissociation of the metastable adduct ions by ejecting $[\text{MC}_6\text{H}_6^+]$ continuously. A detailed discussion will be presented in the kinetic modeling section. Notice that the time scales are significantly different for the $\text{Cr}^+/\text{C}_6\text{H}_6$ and $\text{Mn}^+/\text{C}_6\text{H}_6$ systems. For the $\text{Cr}^+/\text{C}_6\text{H}_6$ system, the ion intensity begins to decrease at ejection times of around $4000 \mu\text{s}$, while the falloff region is around $400 \mu\text{s}$ for the $\text{Mn}^+/\text{C}_6\text{H}_6$ system.

To examine the pressure dependence of the continuous ejection experiments, measurements were carried out at several benzene pressures and also with the introduction of Ar collisional gas at $\sim 9 \times 10^{-7}$ Torr. As seen in Figure 3, the shapes of the ion intensity curves are almost identical when the benzene pressures are below $\sim 4 \times 10^{-7}$ Torr. However, the observed curve shapes start to deviate when the benzene pressure is equal to or above 6×10^{-7} Torr. A further deviation was found when Ar was introduced into the ICR cell at higher pressures ($\geq 6 \times 10^{-7}$ Torr).

Ab Initio Calculations. The full optimized structure and vibrational frequencies of MnC_6H_6^+ were computed using the GAUSSIAN 92 program suite⁴⁴ at the HF/LANL2DZ⁴⁵ level on IBM RS 6000 RISC workstations at the Purdue University Computer Center (PUCC). The optimized structure of MnC_6H_6^+ has C_{6v} symmetry, with six carbons in the same plane and the 6 hydrogens bent slightly out of plane by 2.4° . Mn^+ is above the center of the carbon ring (opposite to the hydrogens) at a distance of 2.608 \AA , which is slightly longer than $r(\text{Cr}^+ - \text{ring})$ by 0.108 \AA . Table 1 gives the vibrational frequencies of MnC_6H_6^+ from the present calculations along with those of CrC_6H_6^+ obtained by Lin and Dunbar.²³

Kinetic Modeling

Mechanism and Kinetics. As shown in eq 1 and Figure 4, newborn adduct ions are metastable, carrying excess internal energy above their dissociation threshold energy. In the absence of a stabilization process (collisional or radiative), and assuming no other reaction channel, the metastable ions, $[\text{MC}_6\text{H}_6^+]$, will back-dissociate to the initial reactants, M^+ and C_6H_6 . Under the low-pressure conditions used in our experiments, the collisional stabilization is slow compared to the back-dissociation rates by about 2 orders of magnitude. Furthermore, the radiative relaxation rates for CrC_6H_6^+ and MnC_6H_6^+ are calculated to be about 35 ± 8 and $18 \pm 5 \text{ s}^{-1}$, respectively.⁴⁶ The metastable ions are too short-lived (a few milliseconds or less) to be observed *directly* in the FT-ICR mass spectrometer, since the ion detection time is usually longer than 1 ms using standard FT-ICR excitation/detection techniques. However, ion ejection times in FT-ICR can be on the same order as metastable lifetimes.

During the constant 8 s reaction time, an rf ejection voltage at a frequency corresponding to the cyclotron frequency of MC_6H_6^+ is continuously applied. Under these conditions, metastable adduct ions may either undergo unimolecular dissociation or be ejected from the ICR cell. If the time required for ion ejection is sufficiently long, most of the $[\text{MC}_6\text{H}_6^+]$ undergo unimolecular dissociation. As a result, the intensity of M^+ will resemble the initial total ion intensity of $[\text{M}^+]$ measured at the same reaction time without the rf ejection voltage applied. However, as the ion ejection time is reduced, the metastable $[\text{MC}_6\text{H}_6^+]$ adducts are ejected from the ICR cell, resulting in a dramatic decrease in the M^+ intensity.

TABLE 1: Vibrational Frequencies for CrC_6H_6^+ and MnC_6H_6^+

species	frequencies (cm^{-1})
$\text{CrC}_6\text{H}_6^{+ a,c}$	$2 \times 56, 126, 2 \times 407, 2 \times 598, 688, 725, 2 \times 892, 936, 987, 2 \times 995, 2 \times 1002, 1016, 1123, 2 \times 1168, 1222, 1353, 2 \times 1451, 2 \times 1563, 3030, 2 \times 3038, 2 \times 3052, 3062$
$\text{MnC}_6\text{H}_6^{+ b,c}$	$2 \times 67, 124, 2 \times 392, 2 \times 595, 672, 729, 2 \times 886, 936, 977, 2 \times 980, 2 \times 1001, 1006, 1133, 2 \times 1169, 1231, 1353, 2 \times 1451, 2 \times 1559, 3034, 2 \times 3041, 2 \times 3055, 3064$

^a Reference 23. ^b Present work. ^c HF/LANL2DZ with frequencies scaled by 0.89.

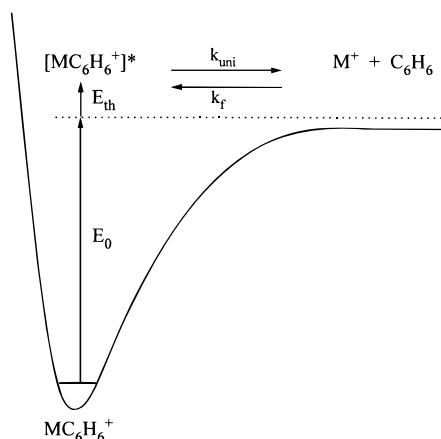


Figure 4. A schematic potential energy surface. E_0 and E_{th} are the dissociation threshold energy and thermal energy of MC_6H_6^+ , respectively.

Therefore, to a first approximation, the time allowed for unimolecular dissociation of $[\text{MC}_6\text{H}_6^+]^*$ is equal to the time required for ion ejection. Thus, in so doing, the *analogous* time-resolved unimolecular dissociation spectrum for the selected metastable ion can be obtained. As shown in Figure 3, a simple exponential fit to the experimental data yields the unimolecular dissociation rates $(1.0 \pm 0.3) \times 10^3 \text{ s}^{-1}$ and $(1.0 \pm 0.4) \times 10^4 \text{ s}^{-1}$ for $[\text{CrC}_6\text{H}_6^+]^*$ and $[\text{MnC}_6\text{H}_6^+]^*$, respectively.⁴⁷ It is gratifying that the value for $[\text{CrC}_6\text{H}_6^+]^*$ is in excellent agreement with the back-dissociation rate of $1.2 \times 10^3 \text{ s}^{-1}$, obtained by Lin and Dunbar from the kinetic analysis of the radiative association reaction between Cr^+ and benzene.²³

RRKM Calculations. A recent publication by Baer and Mayer gives a full description of RRKM modeling from the point of view of practical applications.³² In principle, to relate the measured unimolecular dissociation rates to the benzene/metal ion bond energy, a rate–energy calibration must be established. This was accomplished by adopting the same scheme of kinetic modeling successfully employed by Dunbar and Lifshitz to obtain accurate bond dissociation energies in their time-resolved photodissociation (TRPD) measurements.⁴⁸ The strategy is to extrapolate to zero dissociation rate using a canonical formula of RRKM theory,^{29–31} along with the steepest descents approximation.^{48–50}

Basically, the input parameters for an RRKM calculation include the dissociation threshold energy E_0 and the vibrational frequencies of the precursor ion (MC_6H_6^+ , in the present case) and its corresponding transition state. The vibrational frequencies of CrC_6H_6^+ were obtained from ref 23. The vibrational frequencies of MnC_6H_6^+ were calculated in this work using the same basis set (LANL2DZ) as employed in Ref 23. Since the vibrational frequencies of the transition states are not available, those of the corresponding precursor ions were used to approximate the vibrational frequencies of the transition state with several modifications. Note that the RRKM rate constant is not particularly sensitive to the choice of vibrational frequencies of the transition state, as long as the resulting $\Delta S_{1000\text{K}}^\ddagger$ is consistent with the nature of the potential surface around the

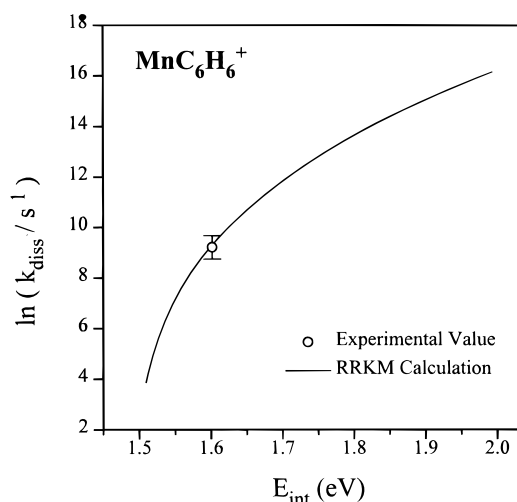
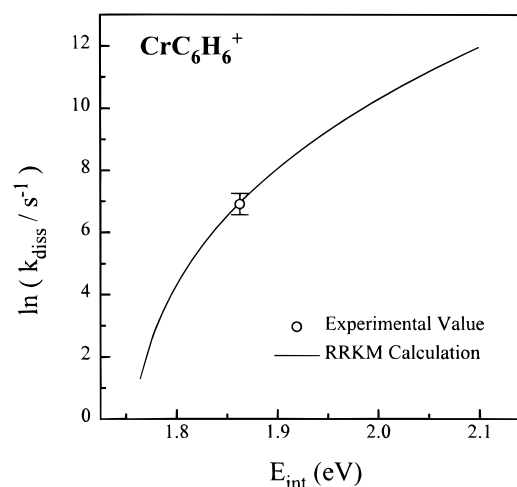


Figure 5. RRKM rate–energy curves and rate–energy points derived from Figure 3. (a) CrC_6H_6^+ and (b) MnC_6H_6^+ .

transition state.⁵¹ This argument has been verified by several research groups.^{48,51}

Normally, the formation of adduct ions occurs through a long-range ion-induced-dipole (or ion-dipole) interaction.¹⁷ Accordingly, the potential energy surface (Figure 4) at the entrance channel is smooth, and the transition state is characterized as a *loose* transition state, which is likely to be a good description for association complexes bound primarily by electrostatic forces.³¹ In general, there is a very positive change in the activation entropy, $\Delta S_{1000\text{K}}^\ddagger$, in going from the associated complex ion to the fragment products for a loose type of transition state. In particular, Dunbar and co-workers have argued that a positive value of +7 eu be assigned for the activation entropy in these types of dissociation processes.⁴⁸

Figure 5 shows the rate–energy curves calculated by RRKM modeling, where the distribution of vibrational energies is assumed to be a Boltzmann distribution. The open circles are the measured unimolecular dissociation rates for CrC_6H_6^+ (Figure 5a) and MnC_6H_6^+ (Figure 5b). Table 2 lists the kinetic parameters used in the RRKM calculations. As shown in Figure

TABLE 2: RRKM Kinetic Parameters

	CrC ₆ H ₆ ⁺	MnC ₆ H ₆ ⁺
ΔS^\ddagger (eu) ^a	+7.0	+7.0
E_0 (eV) ^b	1.75	1.50

^a Assuming a loose transition state, see text and ref 31. ^b Obtained from this work.

4, the total internal energy of the metastable ion is assumed to be the dissociation threshold energy, E_0 , plus the average thermal energy, $\langle E_{th} \rangle$, of MC₆H₆⁺ at 300 K.⁵² Note that this is a simplified kinetic analysis, in which the contribution of rotational energies is not included.⁴⁸ Once the activation entropy has been assigned, the only remaining unknown modeling parameter is the dissociation threshold energy E_0 , which was then treated as an adjustable parameter to bring the calculated rate–energy curve through the experimental rate–energy point.

Discussion

To ensure the validity of the present application of the continuous ejection technique in probing the unimolecular dissociation of metastable ions, several potential complications, including off-resonance ejection, collision-induced dissociation (CID), and collisional stabilization, were carefully examined. To test the effect of off-resonance ejection, the Cr⁺ intensity was monitored by applying an rf voltage (117 V) at several arbitrary values of m/z . It was found that the Cr⁺ intensity was indeed disturbed when the applied radio frequency was within 200 kHz of the cyclotron frequency of Cr⁺ ($\omega_c = 910$ kHz). However, the Cr⁺ intensity was not at all influenced when the applied rf was above 1051 kHz (m/z 45) or below 695 kHz (m/z 68). In the present continuous ejection experiments, the applied rf (the cyclotron frequency of the metastable ion) was well away from the cyclotron frequency of the metal ions. Hence, it is believed that off-resonance ejection did not play a role in the present experiments.

Generally, in order to perform CID experiments, argon pressures of 10^{-6} Torr or above are used.⁵³ Thus, in the present experiments, a pressure of $\sim 4 \times 10^{-7}$ Torr is somewhat low to have a substantial contribution from a CID process. The strongest argument against a contribution from CID is that, if collision-induced dissociation occurred during the ion ejection period, one would expect that the extent of dissociation would increase as the pressure was increased. The experimental curves in Figure 3, however, are almost identical at pressures below 4×10^{-7} Torr. In addition, the unimolecular dissociation of the metastable ions becomes slower in the presence of Ar. Thus, although the possibility of CID cannot be completely excluded in the present experiments, at least the contribution of the metal ion intensity from the CID process does not appear to be significant.

In the kinetic modeling, the total internal energy of the newborn adduct ions is assumed to be equal to the dissociation threshold energy plus the thermal energy of MC₆H₆⁺ at 300 K. The assumption is used to simplify the present kinetic modeling by avoiding the need to consider the collisional stabilization process. However, to ensure the validity of this assumption, experiments must clearly be performed under fairly low-pressure conditions, where collisional stabilization is negligible compared to unimolecular dissociation and ion ejection. As exemplified in Figure 3, the experimental data obtained become pressure independent below $\sim 4 \times 10^{-7}$ Torr and can be fit to a simple exponential function. However, at pressures above 6×10^{-7} Torr, an S-shaped curve was found. According to Anicich's method, the experimental points were fit to a seventh-order polynomial followed by differentiating the polynomial func-

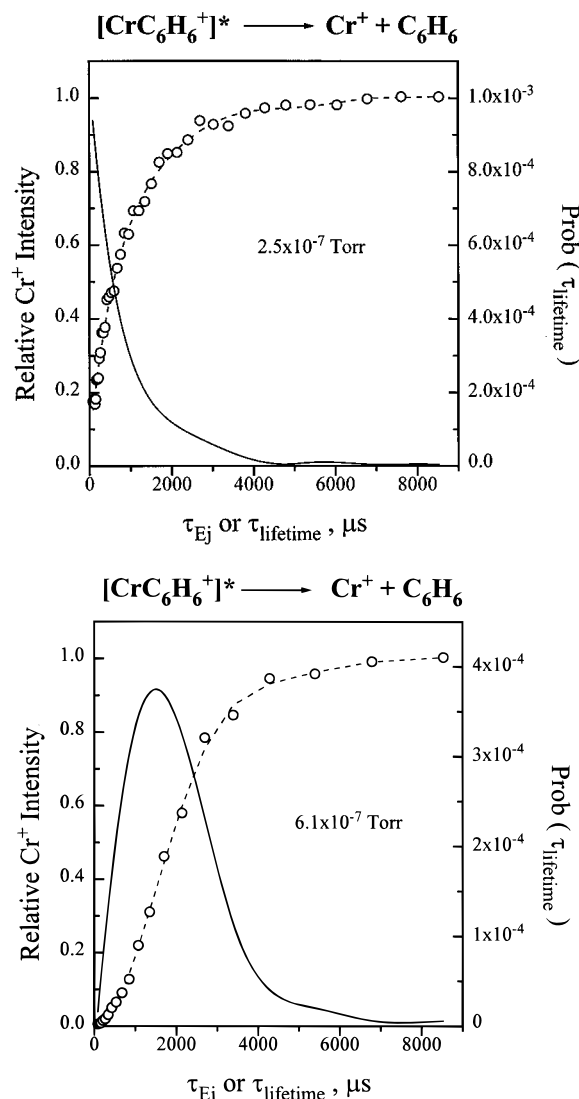


Figure 6. Chromium ion intensity *vs* ion ejection time at a benzene pressure of (a) 2.5×10^{-7} and (b) 6.1×10^{-7} Torr. The dotted lines are fits of the data to seventh-order polynomial functions. The lifetime distributions of [CrC₆H₆⁺]^{*} were derived by differentiating the fitted polynomial functions and are plotted as solid lines.

tion.^{24,25} The resulting lifetime distributions (solid lines) are displayed in Figure 6. Clearly, the lifetime distribution obtained at 2.5×10^{-7} Torr has a finite probability at near zero lifetime and continuously decreases. On the contrary, a peak appears at ~ 2000 μ s for the lifetime distribution obtained at a pressure of 6.1×10^{-7} Torr. This observation suggests that the metastable adduct ions are partially stabilized by additional ion–molecule collisions at a pressure of 6.1×10^{-7} Torr.

As seen in Figure 4, the potential energy surface along the dissociation coordinate is barrierless, based on the assumption of a long-range ion-induced-dipole interaction¹⁷ between the metal ion and neutral benzene. Therefore, the benzene/metal ion bond energy is assigned to be equal to the dissociation threshold energy, E_0 .⁵¹ Table 3 lists the benzene/metal ion bond energies derived from the present work with an uncertainty of ± 0.1 eV. Both bond energies have been previously studied by several methods, including theoretical calculations,⁵⁴ threshold collision-induced dissociation,³³ and kinetic analysis of radiative association reactions.²³ As seen in Table 3, the bond energy values obtained from this study are in excellent agreement with those from the other methods.

As mentioned earlier, the falloff regime begins at ~ 4000 and ~ 400 μ s for CrC₆H₆⁺ and MnC₆H₆⁺, respectively. Also, a

TABLE 3: Bond Dissociation Energies (eV) of $\text{Cr}^+(\text{C}_6\text{H}_6)$ and $\text{Mn}^+(\text{C}_6\text{H}_6)$

$\text{Cr}^+(\text{C}_6\text{H}_6)$	$\text{Mn}^+(\text{C}_6\text{H}_6)$	method
1.63	1.53	theory ^a
1.77 ± 0.1	1.38 ± 0.1	threshold CID ^b
1.72 ± 0.15		RA kinetic method ^c
1.75 ± 0.1	1.50 ± 0.1	continuous ejection ^d

^a Reference 54. ^b Reference 33. ^c Reference 23. ^d Present work.

comparison of parts a and b of Figure 3 shows that the fitted unimolecular dissociation rate of MnC_6H_6^+ is approximately 10 times faster than that of CrC_6H_6^+ . Both observations are consistent with the fact that the benzene/metal ion bond energy of CrC_6H_6^+ is stronger than that of MnC_6H_6^+ . Thus, a desirable property of the continuous ejection technique is that it is quite sensitive to the ligand/metal ion bond energy; furthermore, the agreement between the bond energies derived here and the prior values justifies the kinetic modeling and experimental approach associated with the continuous ejection method.

Despite the successes in deriving accurate metal–ligand bond dissociation energies, thus far, the present kinetic modeling procedures could be further improved. First, a full convolution of the energy distribution would be desirable instead of using a single average thermal energy.⁴⁸ Second, the contributions from both radiative and collisional stabilization processes might be necessary to include. There are also limitations to the types of systems studied by the CE method. While for electrostatically (or even weakly covalent) bound metal–ligand ions the assumption that simple cleavage processes are barrierless along the dissociation coordinate is likely to be correct,³¹ a reverse activation barrier will occur for a dissociation process involving rearrangement. Lastly, as mentioned above, if the mass difference between the reactant ion and the complex ion is less than a few amu, off-resonance effects may result in ejecting the initial reactant ion from the ICR cell unintentionally.

Conclusions

The continuous ejection technique is demonstrated to be applicable to observing the unimolecular dissociation of organometallic metastable adduct ions in the FT-ICR mass spectrometer. Unimolecular dissociation rates of $(1.0 \pm 0.3) \times 10^3$ and $(1.0 \pm 0.4) \times 10^4 \text{ s}^{-1}$ were measured for CrC_6H_6^+ and MnC_6H_6^+ at average internal energies of 1.90 and 1.74 eV, respectively. From the present kinetic analysis, $D^0(\text{Cr}^+-\text{C}_6\text{H}_6) = 1.75 \pm 0.1 \text{ eV}$ and $D^0(\text{Mn}^+-\text{C}_6\text{H}_6) = 1.50 \pm 0.1 \text{ eV}$ were obtained in agreement with the values obtained from threshold CID and radiative association (RA) measurements. The success in obtaining the ligand/metal ion bond energies in this work is greatly encouraging for further applying the continuous ejection experiments to other weakly bound ions and those with few degrees of freedom, which might be difficult using the RA kinetic method. Furthermore, the use of the continuous ejection technique to study organometallic reaction mechanisms is currently underway in our laboratory.

Acknowledgment. This work was supported by the Division of Chemical Sciences in the Office of Basic Energy Sciences in the United States Department of Energy (DE-FG02-87ER13766). The authors also thank Prof. Robert C. Dunbar (Chemistry Department, Case Western Reserve University) for helpful discussions.

References and Notes

(1) Allison, J. *Prog. Inorg. Chem.* **1986**, *34*, 627.

(2) Bowers, M. T., Ed. *Gas Phase Ion Chemistry*; Academic Press: New York, 1979–1984; Vols. 1–3.

(3) Eller, K.; Schwarz, H. *Chimia* **1989**, *43*, 371. Schwarz, H. *Acc. Chem. Res.* **1989**, *22*, 282. Steinrück, N.; Schwarz, H. *Organometallics* **1989**, *8*, 759. Karrass, S.; Prüssse, T.; Eller, K.; Schwarz, H. *J. Am. Chem. Soc.* **1989**, *111*, 9018. Eller, K.; Zummack, W.; Schwarz, H. *J. Am. Chem. Soc.* **1990**, *112*, 621. Schröder, D.; Schwarz, H. *J. Am. Chem. Soc.* **1993**, *115*, 8818. Eller, K.; Schwarz, H. *Chem. Rev.* **1991**, *91*, 1121.

(4) Armentrout, P. B.; Halle, L. F.; Beauchamp, J. L. *J. Am. Chem. Soc.* **1981**, *103*, 6501. Martinho Simões, J. A.; Beauchamp, J. L. *Chem. Rev.* **1990**, *90*, 629.

(5) Russell, D. H., Ed. *Gas Phase Inorganic Chemistry*; Plenum Press: New York, 1989.

(6) Lifshitz, C.; Louage, F.; Aviyente, V.; Song, K. *J. Phys. Chem.* **1991**, *95*, 9298. Lifshitz, C.; Sandler, P.; Grutzmacher, H.-F.; Sun, J.; Weiske, T.; Schwarz, H. *J. Phys. Chem.* **1993**, *97*, 6592.

(7) Freiser, B. S. *J. Mass Spectrom.* **1996**, *31*, 703. Freiser, B. S. *Acc. Chem. Res.* **1994**, *27*, 353. Huang, Y.; Freiser, B. S. *J. Am. Chem. Soc.* **1990**, *112*, 1682. Freiser, B. S. In *ACS Symposium Series: Bonding Energies in Organometallic Compounds*; Marks, T. J., Ed.; American Chemical Society, Washington, DC, **1990**; Vol. 428, p 55. Buckner, S. W.; Gord, J. R.; Freiser, B. S. *J. Chem. Phys.* **1991**, *94*, 4282.

(8) Holland, P. M.; Castleman, A. W. *J. Chem. Phys.* **1982**, *76*, 4195.

(9) Richardson, D. E.; Eyley, J. R. *Chem. Phys.* **1993**, *176*, 457.

(10) Freiser, B. S., Ed. *Organometallic Ion Chemistry*; Kluwer: Dordrecht, 1996.

(11) van der Hart, W. J.; van Sprang, H. A. *J. Am. Chem. Soc.* **1977**, *99*, 32.

(12) Brickhouse, M. D.; Squires, R. R. *J. Am. Chem. Soc.* **1988**, *110*, 2706.

(13) Smith, D.; Adams, N. G. *Int. J. Mass Spectrom. Ion Processes* **1987**, *76*, 307.

(14) Gerlich, D.; Horning, S. *Chem. Rev.* **1992**, *92*, 1509.

(15) Smith, D. *Int. J. Mass Spectrom. Ion Processes* **1993**, *129*, 1.

(16) Herbst, E. *Angew. Chem.* **1990**, *102*, 595. Herbst, E. *J. Chem. Phys.* **1980**, *72*, 5284.

(17) Bates, D. V.; Herbst, E. *Radiative Association*. In *Rate Coefficients in Astrochemistry*; Millar, T. J., Williams, D. A., Eds.; Kluwer Academic Publishers: Dordrecht, 1988, pp 17–40.

(18) Herbst, E.; Dunbar, R. C. *Mon. Not. R. Astronom. Soc.* **1991**, *253*, 341.

(19) Kofel, P.; McMahon, T. B. *J. Phys. Chem.* **1988**, *92*, 6174. Fisher, J. J.; McMahon, T. B. *Int. J. Mass Spectrom. Ion Processes* **1990**, *100*, 701. Tholmann, D.; McCormick, A.; McMahon, T. B. *J. Phys. Chem.* **1994**, *98*, 1156.

(20) Dunbar, R. C. In *Current Topics in Ion Chemistry and Physics*; Ng, C. Y., Baer, T., Poels, I., Eds.; Wiley: New York, 1994; Vol. II, Chapter 5. Cheng, Y.-W.; Dunbar, R. C. *J. Phys. Chem.* **1995**, *99*, 10802. Dunbar, R. C.; Uechi, G. T.; Solooki, D.; Tessier, C. A.; Young, W.; Asamoto, B. *J. Am. Chem. Soc.* **1993**, *115*, 12477. Dunbar, R. C.; Uechi, G. T.; Asamoto, B. *J. Am. Chem. Soc.* **1994**, *116*, 2466. Weddle, G. H.; Dunbar, R. C. *Int. J. Mass Spectrom. Ion Processes* **1994**, *134*, 73.

(21) Klippenstein, S. J.; Yang, Y.-C.; Ryzhov, V.; Dunbar, R. C. *J. Chem. Phys.* **1996**, *104*, 4502.

(22) Dunbar, R. C.; Klippenstein, S. J.; Hrusak, J.; Stockigt, D.; Schwarz, H. *J. Am. Chem. Soc.* **1996**, *118*, 5277.

(23) Lin, C.-Y.; Dunbar, R. C. *Organometallics*, in press.

(24) Anicich, V. G.; Sen, A. D.; Huntress, W. T.; McEwan, M. J. *J. Chem. Phys.* **1991**, *94*, 4189.

(25) Anicich, V. G.; Sen, A. D.; McEwan, M. J. *J. Chem. Phys.* **1994**, *100*, 5 696.

(26) The lifetime of collisional adduct ions is defined by Anicich *et al.* in refs 24 and 25 as the inverse sum of three unimolecular rate constants k_b , k_d , and k_r , where k_d is the reaction rate constant of an additional reaction channel in their studies. Note that, in our case, there is no other reaction channel, but the possible existence of a collisional stabilization process needs to be considered. Thus, k_d is substituted by $k_c[\text{L}]$.

(27) Audier, H. E.; McMahon, T. B. *J. Am. Chem. Soc.* **1994**, *116*, 8294.

(28) van Doorn, R.; Nibbering, N. M. M. *Org. Mass Spectrom.* **1978**, *13*, 527.

(29) Robinson, P. J.; Holbrook, K. A. *Unimolecular Reactions*; Wiley-Interscience: New York, 1972.

(30) Forest, W. *Theory of Unimolecular Reactions*; Academic Press: New York, 1973.

(31) Gilbert, R. G.; Smith, S. C. *Theory of Unimolecular and Recombination Reactions*; Blackwell Scientific Publications: Oxford, 1990.

(32) Baer, T.; Mayer, P. M. *J. Am. Soc. Mass Spectrom.* **1997**, *8*, 103.

(33) Meyer, F.; Khan, F. A.; Armentrout, P. B. *J. Am. Chem. Soc.* **1995**, *117*, 9740.

(34) Cody, R. B.; Kissinger, J. A.; Ghaderi, S.; Amster, J. I.; McLafferty, F. W.; Brown, C. E. *Anal. Chim. Acta* **1985**, *178*, 43.

(35) Gord, J. R.; Freiser, B. S. *Anal. Chim. Acta* **1989**, *125*, 11.

(36) Cody, R. B.; Burnier, R. C.; Reents, Jr., W. D.; Carlin, T. J.; McCreery, D. A.; Lengel, R. K.; Freiser, B. S. *Int. J. Mass Spectrom. Ion*

Processes **1980**, 33, 37. Cody, R. B.; Burnier, R. C.; Freiser, B. S. *Anal. Chem.* **1982**, 54, 96.

(37) Bartmess, J. E.; Georgiadis, R. M. *Vacuum* **1983**, 33, 149. Miller, K. J.; Savchik, J. A. *J. Am. Chem. Soc.* **1979**, 101, 7206.

(38) Grosshans, P. B.; Marshall, A. G. *Int. J. Mass Spectrom. Ion Processes* **1990**, 100, 347.

(39) Comisarow, M. B.; Grassi, V.; Parisod, G. *Chem. Phys. Lett.* **1978**, 57, 413.

(40) Wang, R. C. L.; Ricca, R. L.; Marshall, A. G. *Anal. Chem.* **1986**, 58, 2935.

(41) Kofel, P.; Allemann, M.; Kellerhals, Hp.; Wanczek, K. P. *Int. J. Mass Spectrom. Ion Processes* **1986**, 74, 1.

(42) Lehman, T. A.; Bursey, M. M. Wiley-Interscience: New York, 1976.

(43) Grosshans, P. B.; Marshall, A. G. *Anal. Chem.* **1991**, 63, 2057.

(44) GAUSSIAN 92: Frisch, M. J.; Trucks, G. W.; Head-Gordon, M.; Gill, P. M. W.; Wong, M. W.; Foresman, J. B.; Johnson, B. G.; Schlegel, H. B.; Robb, M. A.; Replogle, E. S.; Gomperts, R.; Andres, J. L.; Raghavachari, K.; Binkley, J. S.; Gonzalez, C.; Martin, R. L.; Fox, D. J.; Defrees, D. J.; Baker, J.; Stewart, J. J. P.; Pople, J. A. Gaussian, Inc., Pittsburgh, PA, 1992.

(45) Hay, P. J.; Wadt, W. R. *J. Chem. Phys.* **1985**, 82, 270.

(46) The formula for the calculations of radiative relaxation rates is

$$k_r(\text{s}^{-1}) = \sum_{i=1}^{N_v} \sum_{n=0}^{\infty} 1.25 \times 10^{-7} n \nu_i^2 (\text{cm}^{-1}) I_i (\text{km/mol}) P_i(n)$$

Details can be found in ref 21.

(47) The unimolecular dissociation rate is obtained by fitting the experimental data in Figure 3 using the following equation:

$$I(t, \text{M}^+) = I(0, \text{ML}^+) (1 - e^{-k_{\text{uni}} t}) + I(0, \text{M}^+)$$

where $I(t, \text{M}^+)$ and $I(0, \text{M}^+)$ are the metal ion intensities at time t and 0; $I(0, \text{ML}^+)$ is the initial ion intensity for the metal–ligand complex ions.

(48) Lin, C.-Y.; Dunbar, R. C. *J. Phys. Chem.* **1994**, 98, 1369. Lin, C.-Y.; Dunbar, R. C. *J. Phys. Chem.* **1995**, 99, 1754.; Dunbar, R. C.; Lifshitz, C. *J. Phys. Chem.* **1991**, 94, 3542. Lifshitz, C.; Levin, I.; Kababia, S.; Dunbar, R. C. *J. Phys. Chem.* **1991**, 95, 1667.

(49) Forest, W.; Prasil, Z. *J. Chem. Phys.* **1969**, 51, 3006.

(50) Forest, W.; Prasil, Z.; Lauren, P. St. *J. Chem. Phys.* **1967**, 46, 3736.

(51) Lifshitz, C. *Adv. Mass Spectrom.* **1989**, 11, 713.

(52) Lifshitz, C. *Adv. Mass Spectrom.* **1978**, 7A, 3.

(53) Armentrout, P. B.; Beauchamp, J. L. *J. Am. Chem. Soc.* **1981**, 103, 784.

(54) Bauschlicher, C. W.; Partridge, H.; Langhoff, S. R. *J. Chem. Phys.* **1992**, 96, 2118.